Pharmaceutical Research, Vol. 24, No. 5, May 2007 (© 2007)
DOI: 10.1007/s11095-006-9211-2

Research Paper

Raman Chemical Imaging for Ingredient-specific Particle Size Characterization of Aqueous Suspension Nasal Spray Formulations: A Progress Report

William H. Doub,[1,4,5] Wallace P. Adams,[2] John A Spencer,[1] Lucinda F. Buhse,[1] Matthew P. Nelson,[3] and Patrick J. Treado[3]

Received September 12, 2006; accepted December 8, 2006; published online March 20, 2007

Purpose. This study was conducted to evaluate the feasibility of using Raman chemical imaging (i.e., Raman imaging microspectroscopy) to establish chemical identity, particle size and particle size distribution (PSD) for a representative corticosteroid in aqueous nasal spray suspension formulations.
Materials and Methods. The Raman imaging PSD protocol was validated using polystyrene (PS) microsphere size standards (NIST-traceable). A Raman spectral library was developed for the active and inactive compounds in the formulation. Four nasal sprays formulated with beclomethasone dipropionate (BDP) ranging in size from 1.4 to 8.3 μm were imaged by both Raman and brightfield techniques. The Raman images were then processed to calculate the PSD for each formulation.
Results. Within each region examined, active pharmaceutical ingredient (API) particles are unambiguously identified and the total number of those particles, particle size and PSD of API free of excipients and PSD of API particles adhered to other excipients are reported.
Conclusions. Good statistical agreement is obtained between the reported and measured sizes of the PS microspheres. BDP particles were clearly distinguishable from those of excipients. Raman chemical imaging (RCI) is able to differentiate between and identify the chemical makeup of multiple components in complex BDP sample and placebo mixtures. The Raman chemical imaging method (coupled Raman and optical imaging) shows promise as a method for characterizing particle size and shape of corticosteroid in aqueous nasal spray suspension formulations. However, rigorous validation of RCI for PSD analysis is incomplete and requires additional research effort. Some specific areas of concern are discussed.

KEY WORDS: drug delivery; nasal; image analysis; spectroscopy; Raman.

INTRODUCTION

Nasal delivery of drug products is becoming increasingly common due to the potential for increased drug uptake rates, improved bioavailability for certain drugs relative to oral dosing, and the convenience of nasal delivery. When conducting product quality studies in support of new drug applications (NDAs) or abbreviated new drug applications (ANDAs), it is relatively straightforward to determine pharmaceutical equivalence of nasal spray products, whereby products are considered pharmaceutical equivalents if they contain the same API(s), are of the same dosage form, route of administration and are identical in strength or concentration. In contrast, assessment of bioequivalence (BE) of nasal drug delivery products is much more challenging.

The approach of the FDA for establishing BE for solution formulations of locally acting nasal sprays and aerosols is to rely on in vitro methods, based on the assumption that *in vitro* studies would be more sensitive indicators of drug delivery to nasal sites of action than would be clinical studies (1). However, the present recommended approach for establishing BE of suspension formulations of locally acting nasal drug products, both sprays and aerosols, is to conduct in vivo studies, despite being time consuming, costly and often inconclusive, in addition to *in vitro* studies. *In vivo* studies are recommended because of the lack of a validated method for characterizing API-specific drug particle size and particle size distribution (PSD) in nasal aerosols and sprays.

This article represents the personal opinions of the authors and does not necessarily represent the views or policies of the US Food and Drug Administration.

[1] Division of Pharmaceutical Analysis, Food and Drug Administration/CDER/OPS, St. Louis, Missouri, USA.
[2] Office of Generic Drugs, Food and Drug Administration/CDER/OPS, Rockville, Maryland, USA.
[3] ChemImage Corporation, 7301 Penn Avenue, Pittsburgh, Pennsylvania 15208, USA.
[4] Division of Pharmaceutical Analysis, Food and Drug Administration, 1114 Market St., St Louis, Missouri 63101, USA.
[5] To whom correspondence should be addressed. (e-mail: william.doub@fda.hhs.gov)

ABBREVIATIONS: API, active pharmaceutical ingredient; BDP, beclomethasone dipropionate; FOV, field-of-view; MCC, microcrystalline cellulose; NIST, National Institute of Standards and Technology; PS, polystyrene; PSD, particle size distribution; LLS, laser light scattering; RCI, Raman chemical imaging.

Although drug particle size distribution (PSD) can be readily determined by a number of methods prior to formulation into a finished product, the primary challenge has been to determine the PSD of the drug substance in the finished nasal aqueous suspension products in the presence of undissolved excipients. Nasal spray suspension formulations typically contain, in addition to the API, suspended microcrystalline cellulose and a number of dissolved excipients, which may include carboxymethylcellulose sodium, polysorbate 80, benzalkonium chloride, edetate disodium, phenylethyl alcohol, dextrose and other ingredients. Excipients such as microcrystalline cellulose typically have a median particle size that is larger than the API. However, excipients often exhibit a broad PSD and a substantial number of excipient particles may exist in the same size range as the drug substance, thus complicating drug substance particle size determination.

To address the limitations of existing PSD methods to support *in vitro* BE studies, a methodology for ingredient-specific PSD determination based on Raman chemical imaging (RCI) technology was investigated. Availability of such a method would equip pharmaceutical scientists with an *in vitro* assessment method that will more reliably determine API-specific PSD of drug substances in finished drug products.

In this paper, we investigate the use of RCI (2–6) in conjunction with brightfield reflectance imaging to measure chemical identity, particle size, PSDs, and particle associations of corticosteroids in an aqueous nasal spray suspension product. Briefly, RCI, a method combining the capabilities of molecular spectroscopy and advanced digital imaging, enables users to detail material morphology and composition with a high degree of specificity in a non-contact, non-destructive manner. An advantage of using Raman chemical imaging is that each pixel in an image has an associated Raman spectrum. Interrogation of individual pixels assists in the interpretation of the data. Presence or absence of API within individual particles can be determined by whether or not the Raman spectral features characteristic of the drug are present.

In the widefield chemical imaging approach used in this work, in which widefield refers to laser illumination of the entire field of view defined by the microscope objective, digital images are acquired at defined Raman scattered spectral features, by imaging multiple sample particles through an electro-optically tunable filter imaging spectrometer. The Raman chemical imaging microscope simultaneously provides diffraction-limited spatial resolution (approaching 250 nm for high signal-to-noise images) and high Raman spectral resolution (<9 cm^{-1}). Alternative Raman imaging technologies based on point mapping (7–11) and line scanning (12,13) are not able to achieve comparable spatial/spectral resolution performance. The no-moving-parts approach employed to construct Raman images enables fusion of optical and Raman chemical imaging data. Fused optical/Raman images are used to guide the differentiation between drug aggregates and individual particles. Validation of the optical/Raman imaging fusion methodology has been performed by characterizing a set of NIST-traceable polystyrene microsphere size standards.

MATERIALS AND METHODS

Materials

Beclomethasone Dipropionate (BDP) aqueous nasal spray was chosen as the focus of this study as it is a commonly used high-dose nasal spray suspension product. A commercial product, Beconase AQ (GSK), was used for initial imaging experiments by brightfield reflectance, polarized light, and Raman techniques. The API, BDP, was supplied by SICOR, S.p.A. (Milan, Italy) as six micronized API samples having volume median particle diameters of 1.4 (lot D), 1.8 (lot E), 2.2 (lot F), 3.4 (lot H, repeated as a blinded duplicate), 8.3 (lot I), and 1.8 (lot J) μm determined at SICOR using laser light scattering (LLS). The particle sizes were blinded to the ChemImage personnel. In addition to API, pure excipient components were examined so as to obtain pure component signature Raman spectra. The inactive components included: microcrystalline cellulose (MCC, Avicel, lot 2130) obtained from FMC Corporation; carboxymethylcellulose sodium (CMC) obtained from KV Pharmaceuticals; dextrose (lot A16A) obtained from Kodak Chemicals; benzalkonium chloride (MCB brand) as a 50% by weight aqueous solution obtained from EM Science; polysorbate 80 (lot 742504) obtained from Fisher Scientific; and phenylethyl alcohol (lot 118PF3435) obtained from Sigma-Aldrich. For validation of the Raman chemical imaging PSD protocol, six NIST-traceable polystyrene (PS) microsphere size standards having mean particle diameters of 0.71, 1.0, 2.1, 5.1, 10 and 32 μm were obtained from Duke Scientific (Duke). Particle size for the smallest particles (0.71 μm) was determined by Duke using transmission electron microscopy. The particle size for all other particles was determined using optical microscopy. Demonstration of RCI PSD analysis was performed on five formulated BDP nasal spray samples. Formulations were prepared at FDA's Division of Pharmaceutical Analysis according to a commercial formulation containing the six excipients indicated above for Beconase AQ. The BDP formulations were provided in spray pump bottles as blinded samples to minimize bias.

Nasal Spray Particulate Preparation

Samples were prepared by shaking, priming (four actuations each) and spraying each nasal spray sample in an upright position onto inverted aluminum-coated glass microscope slides positioned approximately 15 cm from the spray nozzle. The samples were then immediately turned upright and allowed to dry. Aluminum-coated glass microscope slides were used to reduce background response of the detection substrates, including minimizing Raman scatter and background fluorescence typically observed from uncoated glass microscope slides.

Instrumentation

Particle size and particle size distribution measurements were carried out on the API using a Beckman–Coulter LS100Q laser particle size analyzer equipped with a micro-volume accessory. The powder in liquid method was used

with 0.2% Tween 80 (v/v) in water as the suspending agent for obscuration values between 8 and 12% with the stirrer set at 50%. Suspensions were sonicated for 15 min. A 60-s background was collected and data were analyzed according to the Mie model.

Raman spectra, brightfield images, polarized light images and Raman chemical images were obtained using a FALCON™ Raman Chemical Imaging microscope (ChemImage Corporation, Pittsburgh, PA). Raman scattering was achieved by delivering up to 160 mW of 532 nm laser excitation power through a 50X microscope objective to generate a laser spot diameter of 50 μm and a power density of 8.2×10^3 W/cm^2 at the sample. Raman chemical images were collected over an API-specific Raman spectral region at approximately 9 cm^{-1} increments with an average 40 s integration time per image frame. The time required to image a single sample varied depending on the number of sampled FOVs, the integration time per image frame and the total number of image frames. For example, a data set consisting of 50 FOVs at a rate of 40 s per frame for a total of 300 image frames would take approximately 3 h and 20 min to collect. For the formulated nasal spray samples, Raman chemical images were collected and analyzed until at least 100 API particles were counted. To achieve this, surface areas covered for each sample ranged from 39,800 μm^2 (~200 μm×200 μm) to 826,875 μm^2 (~900 μm×900 μm) per sample. Using 2×2 camera binning to enhance image signal to noise ratio, the Raman chemical images exhibited near-diffraction-limited resolution of ~0.3 μm/pixel. The microscope system was calibrated using a 1951 USAF resolution target. The total number of spectra generated for each of the formulated drug samples ranged from 442,225 to 9,187,000. Images were analyzed using ChemImage Xpert™ software.

Detection Protocol

In order to assess the API-specific size distribution in nasal spray product formulations, a systematic methodology was developed.

Step 1. *Collect and analyze Raman spectra of pure ingredients*. A dispersive Raman spectral library was collected for all active and inactive components in the nasal spray product. This analysis was conducted to determine the optimal spectral range to be used during the Raman chemical imaging analysis so as to discriminate the API from other ingredients in the formulation. The spectral range of 1,630–1,700 cm^{-1} was selected on the basis of highest API-specific Raman signal to excipient background ratio. The 1,662 cm^{-1} *C=C* stretching mode of BDP provided the best API to excipient discrimination.

Step 2. *Demonstrate Raman chemical imaging PSD analysis on pure micronized drug substance whose PSD was blinded to the analysts*. Raman chemical imaging was performed by ChemImage personnel on six lots of drug substance provided as blinded samples by FDA personnel. Each sample was prepared by spreading a small amount of micronized BDP on a glass microscope slide to form a monolayer of particles. For each sample, three regions of interest were imaged using brightfield microscopy, polarized light microscopy and Raman chemical imaging. Raman chemical images of the 1,662 cm^{-1} spectral feature were collected and processed to produce a binary Raman image to which an automated particle sizing routine could be applied to generate PSD results.

To produce binary Raman images, the raw image data were preprocessed using a median filter to remove isolated, high intensity pixels characteristic of cosmic ray detection. The data were then bias-corrected to minimize intensity contributions resulting from background fluorescence and detector thermal noise. Subsequently, the Raman image was vector-normalized to minimize contributions from particle surface topography and nonuniformity of response associated with the Gaussian laser illumination profile. The API-specific image at 1,662 cm^{-1} was extracted and Gaussian image noise was reduced using a Wiener-filter noise reduction algorithm (14) prior to applying brightfield image-guided binarization thresholding of the image intensities. Particle size distribution in this study was based on particle chord lengths (maximum distance across a particle).

Step 3. *Demonstrate Raman chemical imaging PSD analysis on a known formulation of aqueous nasal spray suspension*. In separate experiments, formulated samples containing BDP with nominal particle sizes of 1.4, 2.2, 3.4 and 8.3 μm were sprayed onto microscope slides and allowed to dry. For each sample, brightfield, polarized light and Raman chemical images were obtained on identical fields of view. Overlaying these images provided valuable insight into the composition, location and association of particles. These images were processed using ChemImage Xpert™ software to obtain the PSD of the API particles as described above.

Step 4. *Use RCI to measure API particle size in aqueous nasal spray suspension formulations*. Five formulated BDP samples whose PSDs were blinded to ChemImage personnel and marked as 7E1, 8E1, 9E1, 10E1 and 11E1 were provided by FDA personnel. Formulated samples were characterized using the protocol detailed in Step 3. Sufficient non-overlapping fields of view were examined such that at least 100 API particles were counted for each formulation. For single FOV results (such as size standards), particles that crossed the perimeter of the FOV were manually rejected from the particle size analysis. For multiple FOV images (i.e., montages), all particles were included in the analysis. A montage is a composite image comprised of an *X* by *Y* grid of adjacent FOVs that preserve the spatial arrangement of the sample on a larger spatial scale than any single FOV.

Statistical Methods

Statistical analysis was conducted to compare the PSD of the API (maximum chord, Raman) versus the PSD (maximum chord, Raman) of batch formulated with that API. For the formulated products, data for all API particles were used, including those that appeared to adhere to an excipient particle. This is a circumstance where size measurements based on imaging and those obtained from laser light scattering will certainly differ. An API particle attached to

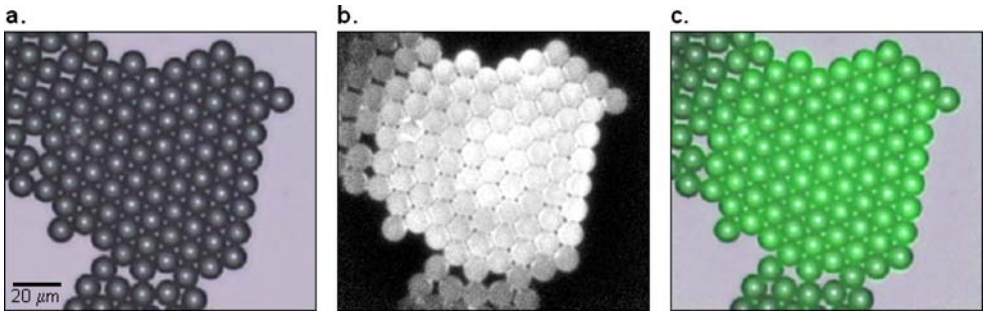

Fig. 1. Brightfield reflectance image (**a**), Raman chemical image (**b**) and brightfield/Raman image overlay image (**c**) of a hexagonally close-packed arrangement of 10 μm, nominal) NIST-traceable polystyrene microsphere size standards.

an excipient particle will appear only as a single large particle in the LLS experiment but chemical imaging will allow those particles to be differentiated. Kolmogorov–Smirnov tests (15) were performed to test for statistically significant differences between two PSDs.

Regression analysis was performed on the mean PSD of API Lots D, F, H and I determined by LLS and the mean PSD of formulated product determined by Raman chemical imaging. Similar analyses were performed on the median and mode summary statistics. These analyses were performed on both untransformed and log-transformed data.

RESULTS

Validation of Raman Chemical Imaging as a Particle Sizing Method

A blinded particle size standard study was performed using six polystyrene (PS) microsphere size standards in order to determine the accuracy of sizing micron dimension particles using RCI and optical microscopy. Initial efforts to characterize isolated, single PS microspheres resulted in a consistent overestimation of particle diameter for both optical and Raman chemical imaging measurements. The systematic overestimates were on the order of 43% for optical imaging and 24% for Raman chemical imaging relative to the particle diameter reported by the supplier. The overestimation in size may be attributable to the difficulty in determining the edge of the spherical particle, especially when approaching the diffraction limit of light (human error). To minimize systematic overestimation, we prepared close packed hexagonal arrays of the microspheres. The resulting particle size can be determined more accurately by measuring multiple PS microspheres in a row and dividing by the total number of spheres, which effectively minimizes edge detection error. This method was used for all PS microsphere studies that formed close-packed arrays.

Using the hexagonal array sizing method, the six different PS standards were prepared by placing small drops of each of the size standard suspensions on standard glass microscope slides and allowing the suspension to dry. Brightfield and RCI measurements were made on particle size standards that formed a hexagonal close-packing arrangement when deposited on a glass microscope slide. Mean particle size and the associated standard deviation were determined as described above. Fig. 1 shows a brightfield reflectance image (a), Raman chemical image (b) and brightfield/Raman image overlay image (c) of a hexagonally close-packed arrangement of 10 μm (nominal) NIST-traceable PS microsphere size standards.

Imaging results for the NIST-traceable particles are shown in Table I. Raman chemical imaging-based sizing results for size standards that formed a hexagonal close-packed arrangement are in good agreement with the nominal NIST-traceable size standard values. A two-sided t test (α=0.05) was performed to determine whether there was a statistical difference between the population means for the Raman measurements compared to the NIST-traceable optical microscopy results. The t test results indicate that there is no statistically significant difference between the mean particle sizes determined by RCI and the NIST-traceable optical sizing method performed by the PS

Table I. Results of Polystyrene Particle Sizing Validation Experiment

NIST-traceable Value (Duke Scientific) (μm)	Original Value: Brightfield Transmittance (ChemImage) (μm)	Original Value: Raman (ChemImage) (μm)	Array Method Value: Brightfield/Raman Overlay (ChemImage) (μm)
0.71±0.01	0.98±0.02	0.9±0.2	0.71±0.01
1.0±0.01	1.9±0.2	1.4±0.2	1.1±0.01
2.1±0.02	3.5±0.1	2.5±0.4	2.1±0.01
5.1±0.5	6.7±1.0*	6.3±0.5*	5.0±0.03*
10.0±0.6	12.2±0.5	12.8±1.3	10.3±0.1
32±2	36±3	35±2	31±1

Values reported are mean ± standard deviation.
* The 5.1 μm size standard did not form close-packed arrays. The mean of three linear subarrays containing two or three particles each is reported.

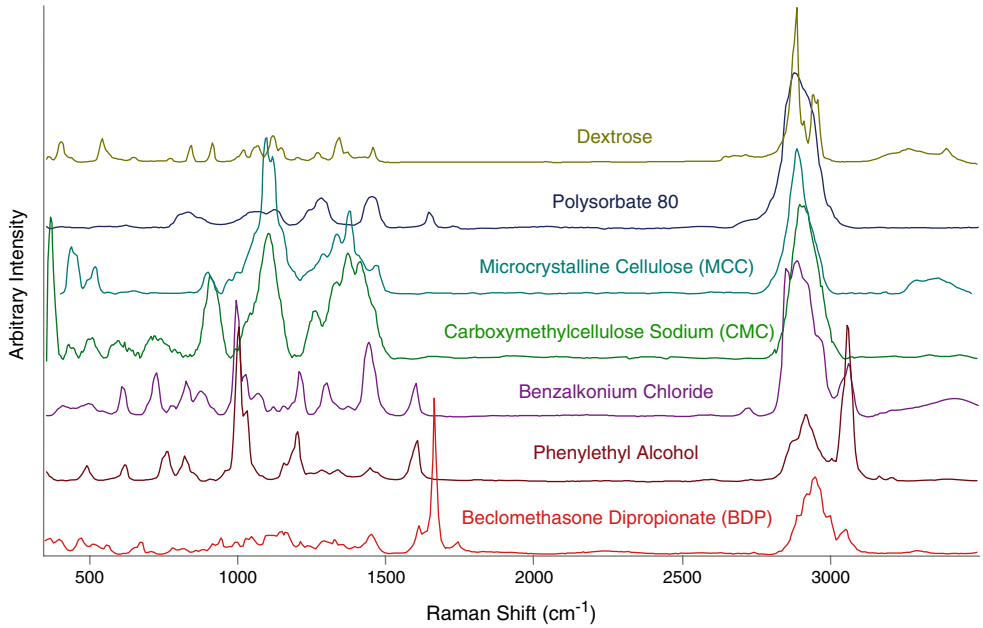

Fig. 2. Overlaid dispersive Raman spectra of all active and inactive ingredients.

microsphere supplier. The validation results shown in Table I are significant in that they demonstrate the feasibility of Raman chemical imaging for quantitative particle sizing. The 5.1 μm NIST traceable size standard could not be sized using the array method as it did not provide the necessary hexagonally close-packed arrangement of PS microspheres. Lack of formation of a close-packed arrangement may be due to the presence of impurities in the sample analyzed although this has not been examined. However, by measuring short "chains" of two to three particles, an average diameter within 2% of the nominal size was obtained.

The overestimation of particle diameter observed here is systematic and can be minimized through appropriate selection of binary thresholding criteria. These criteria may include edge detection based on the optical image where contrast exists and/or based on signal to noise ratios associated with each pixel (i.e., spectrum) in the Raman image. The image analysis procedures refined in the PS

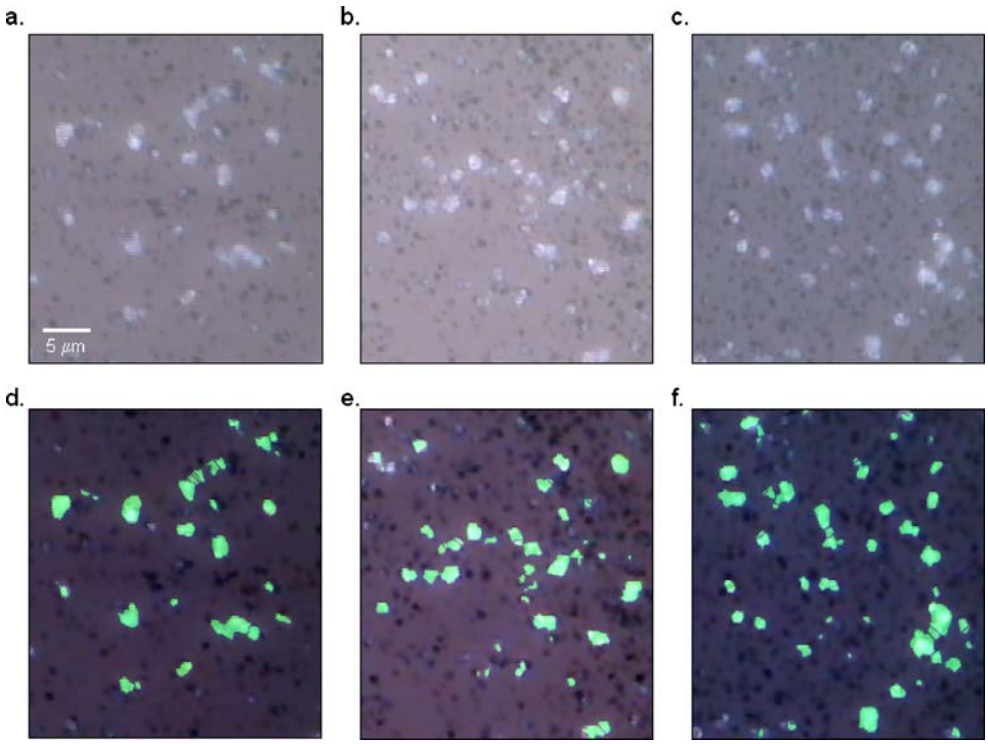

Fig. 3. Brightfield reflectance images (**a**, **b**, **c**) and brightfield/Raman overlay images (**d**, **e**, **f**) from representative fields of view for Lots D, E and F, respectively.

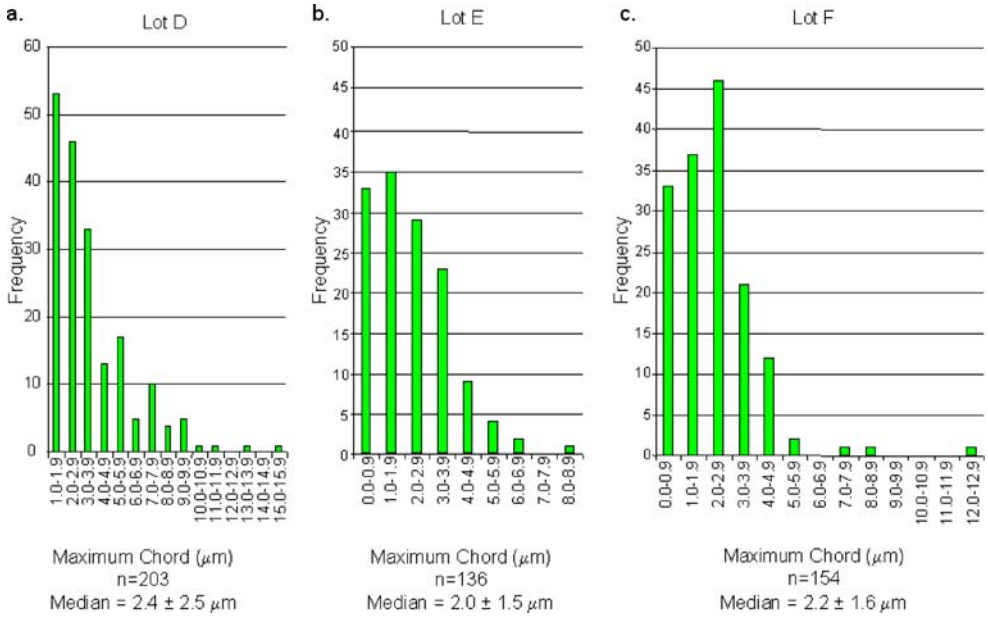

Fig. 4. Raman chemical imaging PSD results of micronized drug based on maximum chord length for Lots D, E and F, respectively.

microsphere array studies led to the use of the optical-image guided protocol for establishing the binarization threshold levels of the API-specific particle sizing data.

Raman Spectral Analysis of Pure Ingredients

Raman spectra were obtained for the API and all excipients present in Beconase AQ nasal spray. Fig. 2 shows the overlaid dispersive Raman spectra of all active and inactive ingredients. These spectra clearly illustrate that each component has a characteristic Raman spectrum that can be used to discriminate between API and other ingredients in the formulated sample. The BDP Raman spectral feature at 1,662 cm^{-1} was selected as the optimal marker to discriminate API from excipients. Other features, as well as the entire spectrum, could have been exploited to generate API-specific Raman image contrast. However, the 1,662 cm^{-1} feature provides adequate discrimination between API and any of the excipients.

Raman Chemical Imaging of Neat Micronized Drug Substance

Raman chemical imaging was performed on six lots of neat micronized drug substance. Fig. 3 shows single field-of-view (FOV) brightfield reflectance images (a–c) and bright-

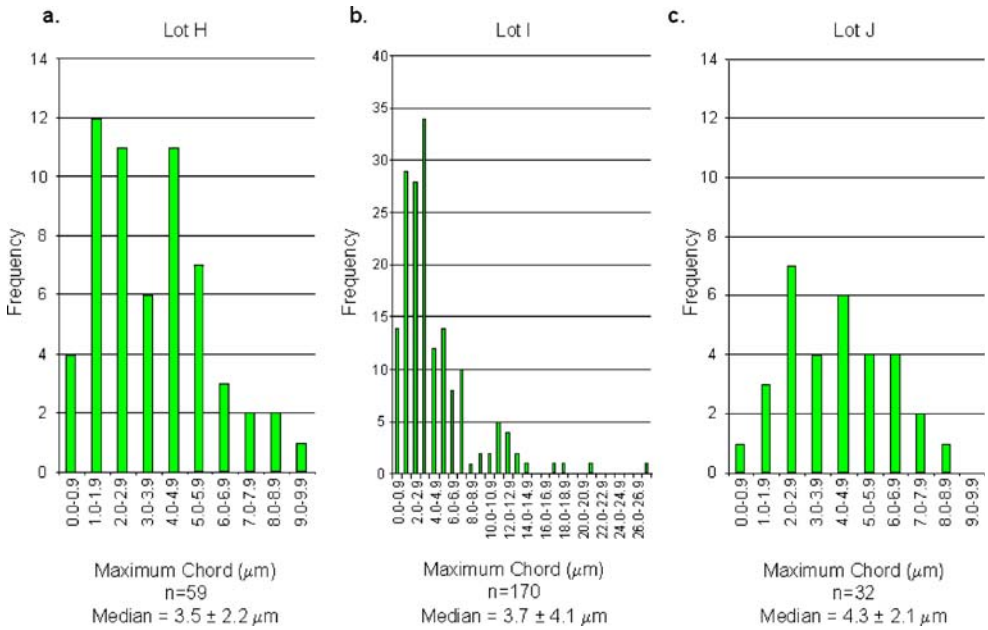

Fig. 5. Raman chemical imaging PSD results based on maximum chord length for Lots H, I and J, respectively.

Table II. Sizing Results Comparison of Micronized (Raman vs. Laser-Light Scattering (LLS)) and Formulated (Raman) API

Micronized API				Formulated API	
API Lot	D_{50}* (μm) (LLS)	Span (LLS)**	Particle Size (Max Chord, μm) (RAMAN)	Formulation Lot	Particle Size (Max Chord, μm) (RAMAN)
D	1.4	2.0	2.4 (SD=2.5, *n*=203)	10E1	2.7 (SD=3.1, *n*=108)
E	1.8	2.0	2.0 (SD=1.5, *n*=136)	NA	NA
J	1.8	5.8	4.3 (SD=2.1, *n*=32)	NA	NA
F	2.2	2.5	2.2 (SD=1.6, *n*=154)	11E1	3.1 (SD=2.6, *n*=124)
H	3.4	3.9	3.5 (SD=2.2, *n*=59)	7E1	1.5 (SD=2.8, *n*=150)
H (duplicate)				8E1	1.2 (SD=3.5, *n*=136)
I	8.3	4.0	3.7 (SD=4.1, *n*=170)	9E1	1.8 (SD=7.0, *n*=103)

SD is the standard deviation, *n* equals number of particles counted. Median particle size is reported to facilitate comparison between LLS measurement results and imaging data.
NA Not applicable: no formulation was prepared using this API lot.
* Volume median diameter
** $(D_{90}-D_{10})/D_{50}$

field/Raman overlay images (d–f) of micronized BDP Lots D, E and F, respectively. Fig. 4 shows the PSD results based on maximum chord length for Lots D, E and F. Fig. 5 shows PSD results based on maximum chord length for Lots H, I and J. These data are summarized in Table II, column 4.

Raman Chemical Imaging of Aqueous Nasal Spray Suspension Control Study

Raman chemical images were collected for a Beconase AQ nasal spray sample. Fig. 6 shows a brightfield reflectance optical image (a), a polarized light image (b) and a brightfield/Raman overlay image (c) of the nasal spray sample for a single region of interest. The green areas in the brightfield/Raman image show the distribution of BDP with respect to other components visible in the brightfield image. The overlay image reveals what appears to be the aggregation of BDP with one or more excipients in the nasal spray sample. Imaging spectrometer Raman signals (d) displayed as color-coded mean spectra are shown from several regions of interest containing particles that exhibit birefringence. We observed that API particles are birefringent. Some other particles, not characterized by RCI, are also birefringent. The Raman spectra clearly reveal the characteristic drug peak for

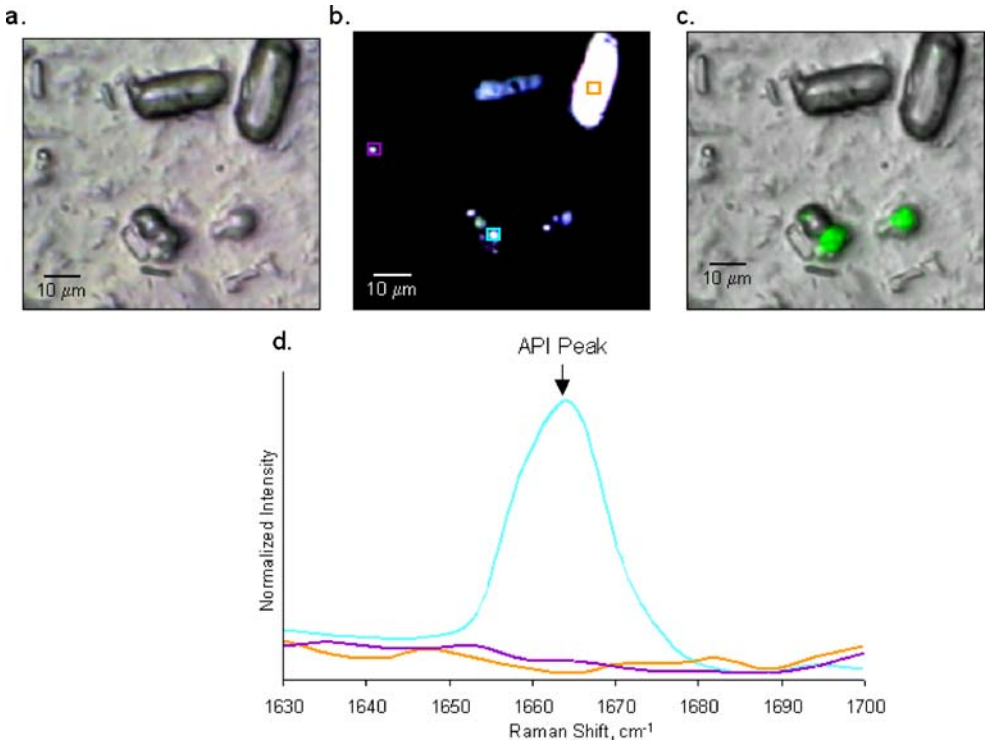

Fig. 6. Brightfield reflectance image (**a**), polarized light image (**b**), and brightfield/Raman overlay image (**c**) of Beconase AQ nasal spray sample for a single region of interest with averaged imaging spectrometer-generated Raman spectra, color-coded to match indicated regions in the polarized light image (**d**).

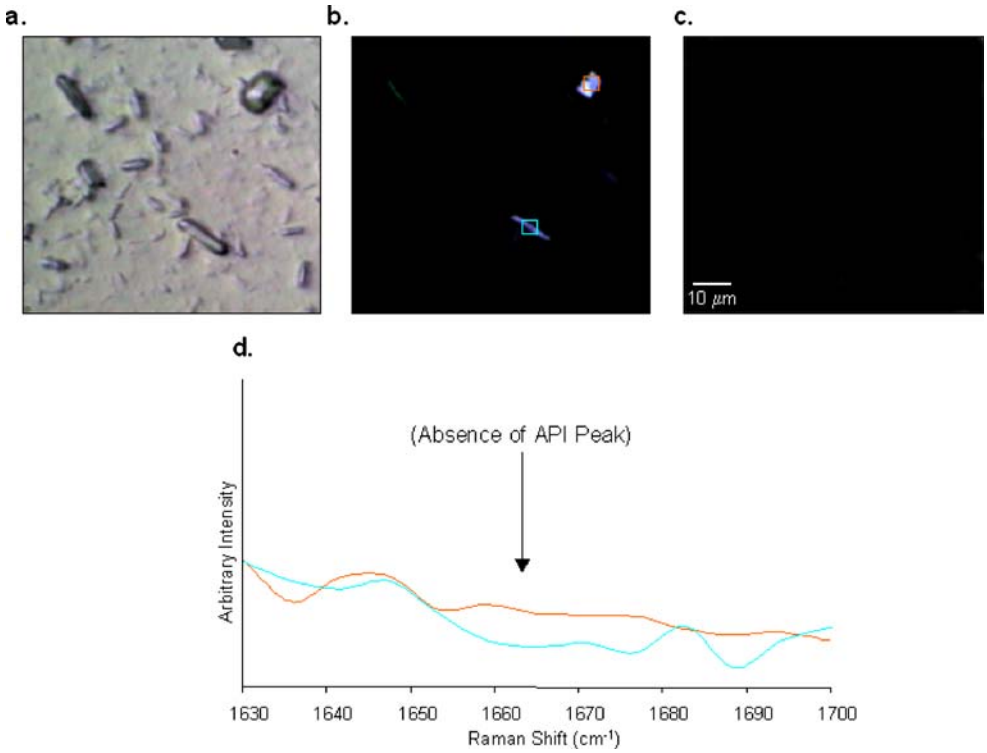

Fig. 7. Brightfield reflectance image (**a**), polarized light image (**b**) and brightfield/Raman overlay image (**c**) of placebo (no API) formulation, color-coded to match indicated regions in the Raman chemical image (**d**).

the drug particles and the absence of the drug peak for other birefringent and non-birefringent components in the sample. As part of the control study, a negative-control (placebo) sample, blinded to the analyst was evaluated. Results are shown in Fig. 7. As would be expected, BDP particles were not detected in the placebo control samples.

Formulated Aqueous Nasal Spray Suspension Blind Study

Five formulated BDP samples were supplied for analysis (7E1–11E1). Fig. 8 shows an example of a single brightfield reflectance image montage out of the two montages collected to characterize LotD/10E1 (a), a binary Raman chemical image montage of the corresponding area (b) and a fused brightfield/Raman chemical image montage of the corresponding area (c). The green pseudo-colored areas in the brightfield/Raman image show the distribution of BDP within the nasal spray excipient background particles. Pseudo-coloring (a virtual staining technique) is based on the characteristic BDP Raman signature. The Raman chemical image montage shown here is comprised of 30 FOVs totaling 958,710 Raman spectra collected at a rate of 35 spectra/s.

The histogram in Fig. 9 describes the particle size distribution for the 108 particles characterized in the LotD/10E1 formulation using RCI. The median drug particle size was determined to be 2.7 μm (SD=3.1). This PSD result is

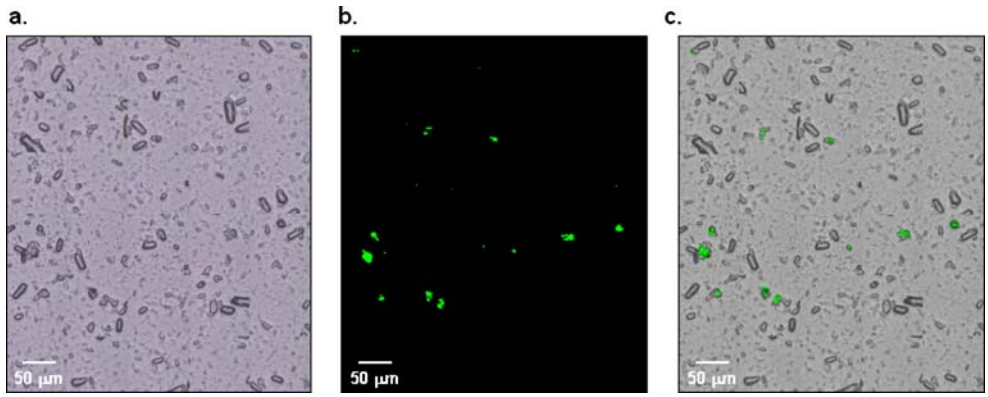

Fig. 8. Brightfield reflectance image montage (**a**), binary Raman chemical image montage (**b**) and brightfield/Raman chemical image montage (**c**) revealing BDP distribution for the LotD/10E1 formulation.

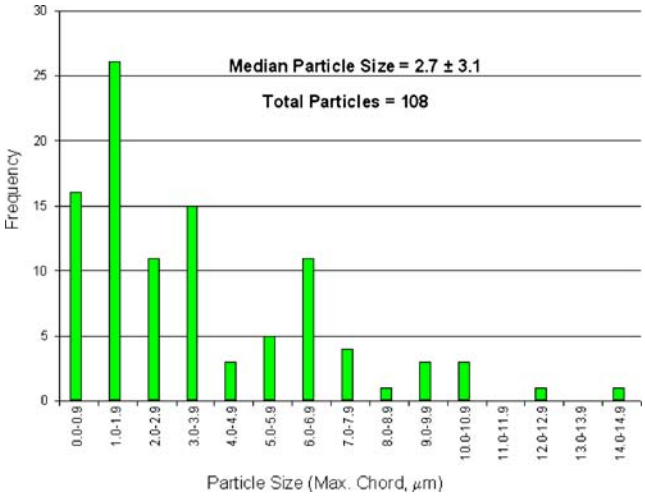

Fig. 9. Total number of particles and maximum chord length-based PSD for the Lot D/10E1 formulation when considering all particles that show as API in the Raman image.

representative of 86 FOVs totaling 2,756,250 Raman spectra. The low particle density observed here is typical of that observed for the sprayed nasal formulation (see, for example, Fig. 6b or c).

Table II summarizes the size data for the neat BDP determined by both LLS and Raman, and for the BDP in the associated formulated aqueous nasal spray suspensions. A priori, similar PSDs between the particle size of the lot of API used to formulate the product and the spectroscopically differentiated particle size of the drug in the formulation was anticipated. Kolmogorov–Smirnov tests revealed statistically significant differences ($p<0.0001$) in PSDs for all comparisons (API Lot F versus formulation 11E1; Lot H versus formulation 7E1; Lot H versus formulation 8E1; Lot I versus formulation 9E1) except Lot D versus formulation 10E1. These results suggest that PSDs differ substantially between the lots of API used to formulate the product and the API from the corresponding lots in the formulated product. API PSD differences observed between pre- and post-formulation samples are not attributable to detection of excipient particles, as RCI exhibits high specificity for API. Regression analyses were performed to examine the relationships between summary statistics (mean, median, and mode) of the four lots of API measured by both LLS and Raman chemical imaging and the respective formulations measured by Raman chemical imaging. Correlation coefficients ranged from 0.07 to 0.85, which in general do not support the a priori expectation that the relative particle size relationship would remain constant.

Assessment of Agglomerated Particles

Due to the high specificity and high spatial resolution capabilities of RCI combined with optical microscopy, direct measurement of the presence of agglomeration (i.e. the cohesion of API and excipient) and the contribution of API to agglomerated particles can be performed. Alternative analytical methods for assessing API PSD do not have this capability. Without an ability to assess the presence and degree of API-excipient agglomeration API PSD is likely to be overestimated. We anticipate that in order to assess *in vitro* BE, it will be necessary to assess the PSD of dispersed and agglomerated API particles, as well as the extent of agglomeration in the nasal spray. For example, it is plausible that micronized API will have reduced availability to nasal sites of action if a significant fraction adheres to excipient or other API particles.

In Fig. 10, API particles that adhere to excipient particles (circled in yellow) are clearly visible when viewed as the Raman/brightfield overlay (a) for the LotD/10E1 formulation. The median PSD of the API was determined to be 2.7 μm (SD=3.0, n=100) for free API particles and 3.1 μm

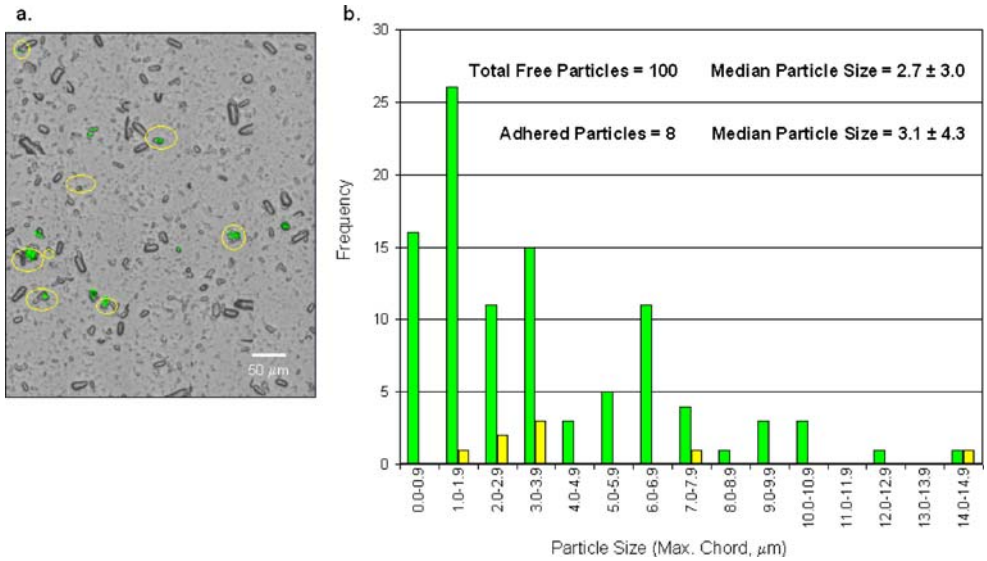

Fig. 10. Binary Raman chemical image (**a**) and maximum chord length-based PSD histogram (**b**) of API particles (*green* bar-free; *yellow* bar-adhered to excipient) that show as API when viewed as the Raman/brightfield overlay for the LotD/10E1 formulation.

Table III. API Particle Association Sizing Results (median max chord, μm)

Formulation Lot	All Particles Containing API	Free API Particles	Adhered Particles
LotH/7E1	1.5 (SD=2.8, *n*=150)	1.5 (SD=2.5, *n*=143)	6.2 (SD=4.5, *n*=7)
LotH/8E1	1.2 (SD=3.5, *n*=136)	1.2 (SD=3.3, *n*=133)	11.0 (SD=1.0, *n*=3)
LotI/9E1	1.8 (SD=7.0, *n*=103)	1.8 (SD=6.8, *n*=96)	6.1 (SD=8.3, *n*=7)
LotD/10E1	2.7 (SD=3.1, *n*=108)	2.7 (SD=3.0, *n*=100)	3.1 (SD=4.3, *n*=8)
LotF/11E1	3.1 (SD=2.6, *n*=124)	3.1 (SD=2.6, *n*=105)	3.1 (SD=2.3, *n*=19)

Values reported as median
SD Standard deviation

(SD=4.3, *n*=8) for adhered particles. Table III shows API particle size data for formulated aqueous nasal spray suspensions in which we tabulate the median size of: (1) all particles containing API; (2) API particles devoid of excipients; and (3) API particles adhered to excipient particles. The larger variance observed for adhered particles may reflect their more irregular shape as compared to free API particles or it may be a consequence of observing only a small number of adhered particles. It should be noted that no optical evidence of API adhering to other API particles is observed. However, this does not preclude the possibility of API particles agglomerating and being detected as a single particle.

DISCUSSION

Raman Spectral Analysis of Pure Ingredients

Raman chemical imaging and spectroscopy has been studied and used for pharmaceutical materials evaluation for many years. The high degree of specificity provided by Raman scattering is well-known (16), and is demonstrated in Fig. 2 in which each component of the nasal spray formulation has a unique Raman spectrum. The uniqueness of the component Raman spectra provides the basis for the underlying specificity of the Raman chemical images.

Validation of Raman Chemical Imaging as a Particle Sizing Method

Using brightfield imaging to guide the thresholding of the Raman chemical images, we have demonstrated the feasibility of using widefield Raman chemical imaging for particle size determination in the particle size range of interest. Fig. 1 shows good agreement between the non-chemical-specific optical brightfield result and chemical-specific Raman chemical imaging result. A two-sided *t* test (α=0.05) evaluation of the data shown in Table I and other size standards ranging between 0.71 and 31 μm (data not shown) indicates that there is no statistically significant difference between the mean particle sizes determined by the array method (brightfield/Raman overlay) and the NIST-traceable sizes supplied by the particle manufacturer.

Raman Chemical Imaging of Neat Micronized Drug Substance

The Raman chemical imaging PSD results from the neat micronized drug substance compare favorably with particle sizing results obtained using laser-light scattering (LLS) for sample lots E, F, H, considering the differences in methodology. Lots D, I and J are less in agreement. The differences observed between the Raman and laser scattering results may be attributed to several causes. First, there are fundamental differences in the mechanisms of the sizing methods. A limitation of the laser scattering method is that the technique assumes a spherical particle shape, while, as can be seen in the optical images of the samples studied here, the particles are often irregular in shape. It is well known that for particles with high aspect ratio, laser scattering results are inherently inaccurate (17,18). Moreover, laser scattering measurements determine size based on a random particle orientation within the sample. In contrast, Raman imaging evaluates a fixed particle orientation deposited on a surface. The Raman imaging measurements are likely to be dominated by preferential particle alignment by which particles lie flat on the substrate following deposition revealing the longest dimension of the particle. Optical evidence observed to date suggests particles do not preferentially align normal to the substrate. Though this does not preclude the possibility, it is not a dominant or even prevalent effect. The imbalance in the number of counted particles between an ensemble method such as LLS and the single-particle method used here may also contribute to the apparent difference between particle sizes. While laser light scattering methods fall into the category of ensemble methods where the properties of the entire distribution within the beam are measured, the Raman microimaging measurements are representative of single particle methods. In the present study, measurements performed on the micronized drug were acquired on as few as 32 particles per drug lot. These counts represent only a small number of FOVs, thus the observed particle size may not be fully representative of the API particles in the sample.

Raman Chemical Imaging of Formulated Aqueous Nasal Spray Suspension

Optical (i.e., brightfield) imaging is highly sensitive but has low intrinsic chemical specificity for classifying API particulate based solely on morphological factors (i.e., particle size and shape). Polarized light microscopy (PLM) may be used to enhance nasal spray particle image contrast and provide additional discrimination capabilities based on the inherent birefringence of the materials. The birefringence can be used for detection of anisotropic crystalline species. However, PLM, like optical reflectance microscopy, is not chemically-specific. As shown in Fig. 6b, API and multiple

excipient particles exhibit varying degrees of birefringence making it impractical to perform chemical identification based on PLM. Both optical microscopy and PLM provide good guidance for subsequent higher chemical specificity detection methods, including RCI. RCI provides a sound basis for discriminating nasal spray ingredients based on the molecular chemical makeup of the individual components. By overlaying brightfield and Raman images as shown in Fig. 6c, quantitative information on the API particle size and degree of association of particles within the formulation can be evaluated. For instance, in Fig. 6c the API adheres to one or more excipients in the nasal spray sample and indicates that RCI may provide a means to investigate changes that may occur in the formulation as a result of the formation of particle agglomerations. This type of information is not obtainable by alternative particle sizing methods.

Formulated Aqueous Nasal Spray Suspension Blind Study

As part of the Nasal Spray Suspension Blind Study, FDA sent ChemImage five lots of formulated material (7E1, 8E1, 9E1, 10E1 and 11E1). Lots 7E1 and 8E1 were formulated from the same lot of API, but this fact was blinded to ChemImage. Statistical comparison of the Raman particle size results (Table II) for these two lots showed them to be the same with a 95% confidence level. Median particle size of the API in the nasal spray formulation determined by RCI did not reveal a rank order relationship with micronized API prior to formulation determined by either LLS or RCI. However, differences between LSS and imaging results are well known (19). Although differences arise primarily because these methods provide different measures of particle size, results from the present study suggest a need for further development of standardized sample preparation prior to chemical imaging. For example, for samples examined by RCI, a collection of microscopic fields of view forming a wedge from spray pattern center to outer edge could be obtained. This would provide a truer representation of the overall particle size distribution within the sample than is obtained from the narrow region of the spray pattern examined in this study. In addition, differences between micronized and formulated API may be due in part to as yet unknown formulation-induced changes. Considerable variability was observed in repeat RCI measurements of micronized drug and formulated product (data not shown). Statistical analyses based on the Kolmogorov–Smirnov test comparing particle size of free API versus API in product also did not reveal a consistent pattern.

CONCLUSIONS

Raman chemical imaging has been evaluated as a method for establishing chemical identity, particle size, and particle size distribution (PSD) characteristics of a representative corticosteroid, BDP, in aqueous suspension of a nasal spray formulation. PSD results collected on polystyrene particle size standards show good statistical agreement between the reported and the measured sizes determined using Raman chemical imaging. Raman dispersive spectral evaluation of corticosteroid nasal spray constituents indicates that Raman spectroscopy has sufficient specificity to discriminate API from excipients, even in complex formulations.

Although it is well understood that LLS and imaging provide different measures of size, our initial expectation was that, given several "lots" of API, rank order of particle size would not be method dependent. However, rank order correspondence was not observed in this study when particle size was measured by the two methods (Table II). Reasons for this may include differences in particle orientation sensitivity between the two techniques and differences in the number of particles measured by each method, i.e., ensemble versus single particle methods.

Results from analysis of formulated nasal sprays demonstrate the ability of RCI to identify the general shape of API, as well as excipients, *in situ* within complex nasal spray formulations recognizing some uncertainty of shape where agglomeration occurs. By fusing brightfield optical imaging and RCI, the technique also provides valuable insight into the association of particles and has the potential to provide unique information on API-excipient agglomeration.

While the goals of providing chemical differentiation, particle size and particle size distribution in aqueous nasal spray suspension products have not been fully realized, RCI holds promise to provide this essential information. Inconsistency in measured particle sizes between micronized and formulated API, along with high variability associated with replicate measurements, is observed. Additional analytical method development including sample preparation, increased automation to enable measurement of a greater number of particles, incorporation of more representative sampling, and investigation of possible formulation-induced changes in particle size are necessary for RCI to attain those goals.

ACKNOWLEDGEMENTS

We would like to thank Giancarlo De Servi (SICOR S.p.A., Milan, Italy) for the gift of micronized BDP, FMC BioPolymer (Newark, DE) for the gift of Avicel RC-591, Joseph Vasiliou (Duke Scientific) for the recommendation to use packed arrays to accurately estimate particle size of polystyrene standard particles, and Qian H. Li, Mathematical Statistician, FDA/CDER/Office of Biostatistics, for the conduct of statistical analyses. We would also like to thank the reviewers of this paper for their excellent comments.

REFERENCES

1. U.S. Department of Health and Human Services, Food and Drug Administration, Center for Drug Evaluation and Research. April 2003, *Draft Guidance for Industry, Bioavailability and Bioequivalence Studies for Nasal Aerosols and Nasal Sprays for Local Action*.
2. H. R. Morris, C. C. Hoyt, P. Miller, and P. J. Treado. Liquid crystal tunable filter Raman chemical imaging. *Appl. Spectrosc.* **50**:805–811 (1996).
3. H.R. Morris, J F. Turner II, B. Munroe, R. A. Ryntz, and P. J. Treado. Chemical imaging of Thermoplastic Olefin (TPO) surface architecture. *Langmuir* **13**:2961–2972 (1999).
4. M. P. Nelson, C. T. Zugates, P. J. Treado, G. S. Casuccio, D. L. Exline, and S. F. Schlaegle. Combining Raman chemical imaging and scanning electron microscopy (SEM) to characterize ambient fine particulate matter. *Aerosol Sci.Tech.* **34**:108–117 (2001).

5. P. J. Treado, and M. P. Nelson. Raman imaging, handbook of Raman spectroscopy. In I. R. Lewis and H. G. M. Edwards (eds.), Marcel Dekker, Inc., New York, 2001, pp. 140–159.
6. C. T. Zugates and P. J. Treado. Raman chemical imaging of pharmaceutical content uniformity. [http://www.ijvs.com] *Int. J. Vibr. Spectrosc*. **2**:4 (1999).
7. L. C. Boogh, R. J. Meier, and H. H. Kausch. A Raman microscopy study of stress transfer in high-performance expoxy composites reinforced with polyethylene fibers. *J. Polym. Sci., B, Polym. Phys.* **30**:325–333 (1992).
8. S. P. Nadula, T. M. Brown, R. W. Pitz, and P. A. DeBarber. Single-pulse, simultaneous, multipoint, multispecies Raman measurements in turbulent nonpremixed jet flames. *Opt. Lett.* **19**:414–416 (1994).
9. X. M. Yang, K. Ajito, D. A. Tryk, K. Hashimoto, and A. Fujishima. Two-dimensional surface-enhanced Raman imaging of a roughened silver electrode surface with adsorbed pyridine and comparison with AFM images. *J. Phys. Chem.* **100**:7293–7297 (1996).
10. C. M. Stellman, K. S. Booksh, and M. L. Myrick. Multivariate Raman imaging of simulated and "Real World" glass-reinforced composites. *Appl. Spectrosc.* **50**:552–557 (1996).
11. D. F. Steele, P. M. Young, R. Price, T. Smith, S. Edge, and D. Lewis. The potential use of Raman mapping to investigate *in vitro* deposition of combination pressurized metered-dose inhalers. *AAPS J*.**6**:4 (2004).
12. M. Bowden, D. J. Gardiner, G. Rice, and D. L. Gerrand. Line-scanned micro Raman spectroscopy using a cooled CCD imaging detector. *J. Raman Spectrosc.* **21**:37–41 (1990).
13. N. L. Jestel, J. M. Shaver, and M. D. Morris. Hyperspectral Raman line imaging of an aluminosilicate glass. *Appl. Spectrosc.* **52**:64–69 (1998).
14. J. Lim. *Two-dimensional signal and image processing*, Prentice-Hall, Upper Saddle River, NJ, 1990.
15. W. W. Daniel. *Applied Nonparametric Statistics*, 2nd ed. PWS-KENT Publishing Company, Boston, (1990), p. 330.
16. J. M. Chalmers and P. R. Griffiths (eds.), Handbook of Vibrational Spectroscopy, Wiley, New York, 2002.
17. M. Levin. Particle characterization—tools & methods. *Lab. Equip*. **42**(7):12–14 (2005).
18. M. Levin. Sizing particles. *Am. Lab. News* **37**(23):14–15 (2005).
19. R. N. Kelly. False Assumptions: Laser Diffraction PSA Systems Exposed. http://www.particlesize.com/Bibliography/false%20with%20notes.pdf (Accessed 11/30/2006).